Solid State ^{13}C CP-MAS NMR Studies of the Crystallinity and Morphology of Poly(L-lactide)

Khalid A. M. Thakur,* Robert T. Kean, John M. Zupfer, and Nancy U. Buehler

Cargill Incorporated, Central Research, P.O. Box 5699, Minneapolis, Minnesota 55440

Matthew A. Doscotch and Eric J. Munson*

Department of Chemistry, University of Minnesota, 207 Pleasant Street SE, Minneapolis, Minnesota 55455

Received June 6, 1996; Revised Manuscript Received September 17, 1996[⊗]

ABSTRACT: Solid-state ^{13}C CP-MAS NMR spectroscopy has been used to investigate highly crystalline, partially crystalline, and amorphous poly(L-lactide) (PLLA). The amorphous domains have broad resonances with Gaussian line shapes, while the crystalline domains have narrower resonances with a high degree of Lorentzian character. Spectra of highly crystalline PLLA have at least five distinct resonances for the carbonyl and methine functional groups in the polymer, indicating five or more crystallographically inequivalent sites in the crystalline domains of the polymer. For the amorphous polymer, broad Gaussian peaks are observed for each of the methyl, methine, and carbonyl functional groups. Spectra of partially crystalline PLLA contains spectral features of both domains, and furthermore, the spectra appear to be sensitive to both *short range* (nanometer) and *long range* (micrometer) order within the polymer. A method to extract the information of crystallinity and morphology from the solid-state CP-MAS NMR spectra of partially crystalline PLLA is discussed.

Introduction

Lactic acid based aliphatic polyesters are well-known bioresorbable polymers which are increasingly being explored as an alternative to nondegradable bioresistant polymers.[1] The nondegradable polymers are generally produced from nonrenewable resources like crude oil and natural gas and are becoming a source of ecological problems due to the huge amount of wastes generated from the 70 million tons of polymers produced each year in the world.[1] The poly(L-lactide) formed from L-lactic

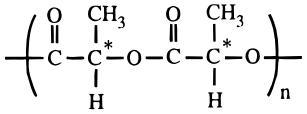

Poly(lactide)

acid produced from natural renewable sources (e.g. corn) decomposes rapidly and completely in a typical compost environment. This makes it an ideal replacement for nondegradable polymers in numerous applications like yard-waste bags, food containers, etc.

Lactic acid possesses one asymmetric carbon and exists in two configurations, *R* and *S*. The lactic acid produced from corn contains predominantly the *S* stereoconfiguration which in comparison to L-glyceraldehyde is also referred to as L-lactic acid. Poly(lactide) polymer is formed by ring opening polymerization[2] of lactic acid cyclic dimers (lactides) which exist as either *RR*, *SS*, or *RS* configuration. The *RR* configuration of the cyclic dimer is sometimes referred to as D-lactide while *SS* configuration is referred to as L-lactide. An equimolar ratio of *RR*- and *SS*-lactide is referred to as *racemic*, and the *RS*-lactide is referred to as the *meso* monomer. High-purity *RR*- and *SS*-lactides form stereoregular (*isotactic*) poly(D-lactide) (PDLA) and poly(L-lactide) (PLLA) respectively, which readily crystallize to a form with high melting point (∼190 °C)[3−6] and glass transition temperature (T_g) of around 60 °C. The *meso* monomer on the other hand, forms *atactic* poly(D,L-lactide) which does not crystallize.[6−8]

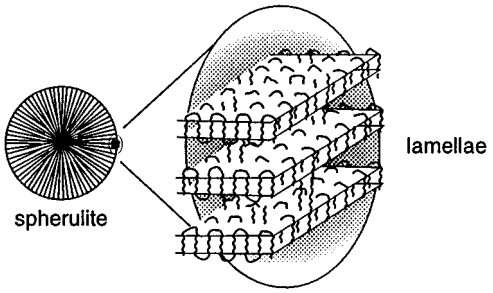

Figure 1. Simple schematic of the various levels of morphology in PLLA. The lamellae in the spherulites are comprised of 10_3 helical chains stacked together in a well-ordered lattice. The folds, interlamellar links, and chains adsorbed on the surface comprise the "partially ordered" and disordered amorphous domains separating the lamellae.

The percent crystallinity and microscopic morphology of PLLA varies with its thermal history (e.g. annealing),[9] amount and type of additives,[10] and stereosequence distribution (e.g. *S*-length distribution). The crystalline domains grow as spherulites from nucleation sites with the amorphous component present in between each of the spherulites.[9−11] Each spherulite is formed by lamellae growth in all directions. The lamellae are formed by helical PLLA chains stacked normal to the lamellae growth with each chain folding back on itself at regular intervals.[12,13] Some of the lamellae may have uncrystallized polymer chains adsorbed on the surface of chain folds.[13] A few interlamellar links and unresolvable entanglements may also be present.[13] The polymer morphology is pictorially depicted in Figure 1. From theories of polymer chain folding, the lamellar thickness is expected to be dependent on the crystallization temperature.[13−15] In PLLA, if the defects of -*R*- (from *meso*-lactide) and -*RR*- (from D-lactide) stereocon-

* Authors to whom correspondence should be addressed.
⊗ Abstract published in *Advance ACS Abstracts,* December 15, 1996.

S0024-9297(96)00828-5 CCC: $12.00

figuration are rejected from the crystalline domains, the lamellar thickness will be reduced.[14] Furthermore, since there is a distribution of *S*-lengths in the polymer, some fraction of the defects may be incorporated into the crystalline domains.[15] As a consequence, the heat of crystallization measured by DSC may also depend on the stereosequence distribution in the polymer.[14] The conformation of the helices in quiescently crystallized PLLA have been shown to be 10_3 (α-form) in a number of studies of thin films and fibers.[5,16,17] Another crystal form (β) with a 3_1 helical conformation is known to form only when PLLA is crystallized under stress.[5,16,17] Talc which is commonly added as a filler also acts as a nucleating agent and increases the number of spherulites. It is important to determine the percent crystallinity ($\%\chi_c$) and morphology, since it strongly influences the physical characteristics of the polymer.[18] A number of techniques can be used to analyze the polymer including DSC and WAXS to estimate the $\%\chi_c$ and polarized microscopy and SAXS to determine the morphology.[9,11]

Solid-state NMR techniques that have been used to estimate the crystallinity in polymers include, T_1, $T_{1\rho}$, and T_2 measurements, multiple quantum coherence spectroscopy, and deconvolution of resonances in proton-decoupled NMR spectra.[19−24] In this paper we show that room temperature (∼22 °C) ^{13}C CP-MAS NMR spectra of partially crystalline PLLA ($T_g \sim 60$ °C) also contain quantitative information about $\%\chi_c$ and morphology. Since NMR is sensitive to short-range order (nanometer), regularity of the environment around the probed nuclei affects the observed spectral line width. The nuclei in the disordered amorphous domains have a large number of possible environments. This leads to a distribution of NMR chemical shifts, resulting in a broad Gaussian line shape for its spectral absorption. On the other hand, the nuclei in the crystalline component have a restricted range of environments, giving rise to narrower spectral line widths. The molecules in the folds do not possess this restricted crystalline three-dimensional environment but have a range of environments. The molecules in the crystalline lattice near the surface of each lamellae also have a nonuniform environment. As the lamellar thickness reduces, the relative spectral contribution from the molecules near the surface increases. Hence, the spectral line widths are expected to increase with decreasing lamellar thickness. Additives like talc also create a nonuniform environment for molecules near their surface which can lead to broadening of the spectral resonances. Furthermore, we have found the line width of the crystalline peaks in ^{13}C CP-MAS spectra of partially crystalline PLLA to also be correlated with the presence of *R* stereoconfiguration defects in the polymer and the average spherulite size. A simple method to deconvolute the NMR spectra and extract the information about percent crystallinity and average morphology is discussed.

Experimental Section

Materials. All poly(lactide) samples were provided by Cargill Corn Milling EcoPLA Development Group. The almost pure (>99.9%) Poly(L-lactide) (PLLA) was polymerized and crystallized at 130 °C in a vial for 1 week. Large spherulites were observed in this sample. Other PLLA samples which were polymerized with various fractions of *meso*-lactide and D-lactide monomer impurities in a pilot plant were melted and rapidly cooled ("quenched") to room temperature. Part of each sample was "melt-crystallized" by reheating to 200 °C and then annealing for 2 h at 130 °C. Two samples were "quench/annealed" by subjecting the quenched polymer to annealing at 130 °C for 2 h. Talc was also present (1% and 10% by weight) in some of the samples. The quenched samples are expected to be mostly amorphous, while the annealed samples are expected to possess varying amounts of crystallinity. The samples are listed in Tables 1 and 2. The samples in Table 2 were prepared under highly controlled conditions, and a thin film of the sample was simultaneously prepared for analysis by polarized microscopy.

Table 1. List of PLLA Samples Melt-Crystallized at 130 °C

no.	% *R*	% talc	ΔH_{cryst} (J/g)	$\%\chi_c$ (by linear fit)[a]
1	<0.1	0	98.40	
2	1.6	0	48.89	53
3	1.6	1	51.37	57
4	1.6	10	47.87	49
5	3.2	0	34.50	38
6	3.2	1	36.90	40
7	3.2	10	32.02	33
8	6.3	0	24.01	15
9	6.3	1	28.99	31
10	6.3	10	26.33	23

[a] $\%\chi_c$ is the fraction of crystalline resonance required for the fit and includes the contribution from molecules in the chain folds at the surface of lamellae.

Table 2. List of PLLA Samples with Thin Film Analysis

no.	% *R*	% talc	thermal history	ΔH_{cryst} (J/g)	$\%\chi_c$ (by linear fit)[a]	data points averaged[b]
1	1.6	0	quenched	0.91		
2	1.6	0	melt-crystallized	53.09	69	±8
3	1.6	0	quench/annealed	43.00	56	±10
4	1.6	1	quenched	2.14		
5	1.6	1	melt-crystallized	52.43	69	±10
6	1.6	1	quench/annealed	37.71	50	±12

[a] $\%\chi_c$ is the fraction of crystalline resonance required for the fit and includes the contribution from molecules in the chain folds at the surface of lamellae. [b] The numbers represent *n* in the (2*n* +1) "moving average" of data points carried out to represent broadening of the crystalline resonance in the *linear combination fit* to data.

The % *R* content in each of the polymer samples was measured by HPLC as % D-lactic acid after complete hydrolysis of the polymer. This measured *R* stereoconfiguration content is expected to be from almost equal amounts of D-lactide and *meso*-lactide in the polymer.

Methods. DSC. The crystallinity of samples was determined as $\Delta H_{cryst} = \Delta H_{exothermic} + \Delta H_{endothermic}$ by DSC using a Mettler DSC30. $\Delta H_{exothermic}$ is observed (between 80 and 150 °C) if the polymer crystallizes during the DSC scan. By definition, $\Delta H_{endothermic}$ is positive and $\Delta H_{exothermic}$ is negative. Samples (10 mg) were scanned from −20 to 200 °C at a rate of 20 °C/min. The cutoffs for assignment of the slope of baseline and for integration of the endothermic and exothermic peaks were subjectively assessed and can lead to error in the calculated ΔH values. In addition, the reported values of ΔH_{cryst} have neither been corrected for the presence of talc nor for effects due to variations in % *R* stereoconfiguration content.

Polarized Microscopy. Some of the samples were also made into thin films and annealed under identical conditions. Photographs of their morphology were taken with a 35 mm camera mounted on a cross-polarized light microscope at a total magnification of 100×.

NMR Spectroscopy. All solid-state NMR spectra were acquired on a Chemagnetics CMX-2 300 MHz spectrometer operating at 75.4 MHz for ^{13}C using cross polarization (CP), magic-angle spinning (MAS), and high-power (>50 kHz) ^{1}H decoupling. A Chemagnetics double-resonance probe with a Vespel spinning module housing a 7.5 mm (0.4 cm^3 sample size) zirconia rotor with Kel-f drive tip and end caps was used.

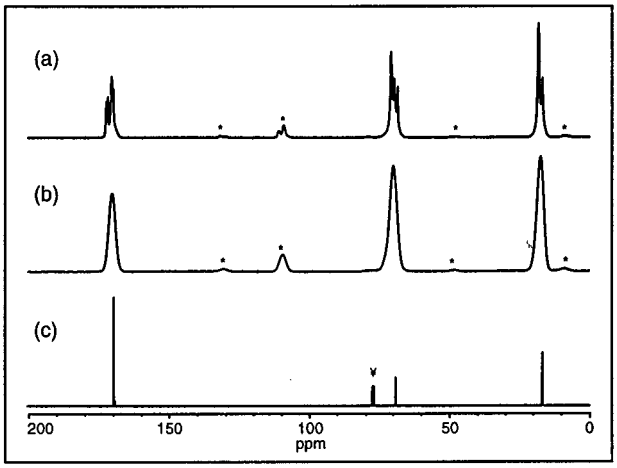

Figure 2. (a) ^{13}C CP-MAS spectrum of partially crystalline 1.6% *R* PLLA, (b) ^{13}C CP-MAS spectrum of amorphous 1.6% *R* PLLA, and (c) ^{13}C solution NMR spectrum of 5% *R* PLLA as 10% solution in $CDCl_3$. The peaks marked by * are spinning sidebands which are artifacts of MAS. The peaks marked by ¥ in the solution NMR spectrum are due to $CDCl_3$ solvent.

All spectra were acquired at a MAS speed of 4.5−4.6 kHz, contact time of 3 ms, and recycle time between subsequent acquisitions of 3 s. Between 512 and 2048 data points were acquired using a spectral width of 30 kHz, corresponding to acquisition times of 17 to 68 ms, respectively. A total of 1024 transients were typically averaged for each sample.

The ^{13}C solution NMR spectra were acquired on a Varian 300 MHz NMR spectrometer at 75.4 MHz with proton decoupling. A total of 64 000 data points were acquired at a spectral width of 20 kHz corresponding to an acquisition time of 3.2 s. The recycle time was set at 1 s, and 4000 scans were averaged.

Linear Combination Fit. The carbonyl resonance of a partially crystalline PLLA sample was fit by a linear combination of the experimentally observed resonance for a highly crystalline PLLA sample and the observed resonance for an amorphous PLLA sample. In order to perform this data analysis, the spectra containing the three resonances with identical spectral width and data points were transferred to a graphing spreadsheet. Since the cross-polarization efficiency for the amorphous and crystalline PLLA samples was found to be identical (*vide infra*), the area of all the resonances was normalized to 10^6 arbitrary units. In order to accurately simulate the line widths of the partially crystalline sample, the carbonyl resonance of the highly crystalline PLLA was artificially broadened by averaging adjacent data points. This simple "moving average" of $(2n+1)$ data points is an approximation to Gaussian broadening. The fit was generated as a linear combination of the broadened resonance of highly crystalline PLLA and the resonance of amorphous PLLA. This fit was then plotted on the same scale as the resonance of the partially crystalline resonance and the accuracy of the fit was visually assessed. There were only two variables in this *linear combination fit, viz.* the fraction of highly crystalline resonance used and the number of data points averaged. These two variables were altered until a good fit was visually determined. In principle, a computer program could be written to perform a linear least squares fit using the two variables.

Results and Discussion

Figure 2 shows the ^{13}C CP-MAS NMR spectrum of a partially crystalline ("melt-crystallized") 1.6% *R* PLLA sample, the ^{13}C CP-MAS spectrum of an amorphous ("quenched") 1.6% *R* PLLA sample, and the proton-decoupled ^{13}C NMR spectrum of 3.6% R PLLA as 10% by weight solution in deuterated chloroform. As expected, the solution NMR resonances are significantly narrower than the solid-state NMR resonances. The ^{13}C resonances at approximately 17, 70, and 170 ppm correspond respectively to the methyl, methine, and carbonyl carbons in the polymer. The small peaks in the CP-MAS spectra around 5, 50, 110, and 130 ppm are spinning sidebands which are artifacts of magic-angle spinning (MAS). The CP-MAS NMR resonances of each of the carbon groups in the partially crystalline PLLA are split into 3−5 distinct peaks. The amorphous sample has broad spectral resonances with Gaussian line shapes. The carbonyl resonance in the amorphous sample is a Gaussian peak centered at ∼170.2 ppm, while the methine and methyl carbon resonances can each be deconvoluted into two Gaussian peaks centered at ∼69.8 and ∼73 ppm and at ∼17 and ∼18.6 ppm, respectively.

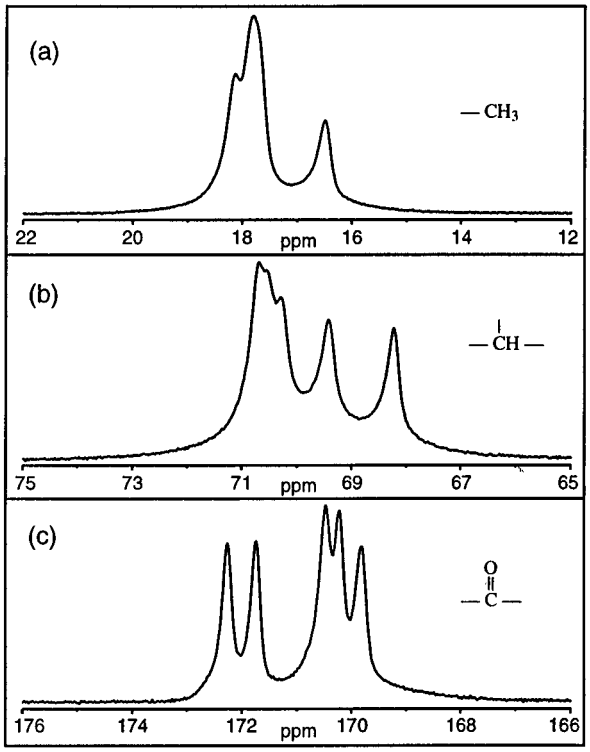

Figure 3. ^{13}C CP-MAS spectra of (a) methyl, (b) methine, and (c) carbonyl resonances of a highly crystalline PLLA with less than 0.1% *R*-lactide content.

The methyl, methine, and the carbonyl resonances in a highly crystalline PLLA sample with less than 0.1% *R* content are shown in Figure 3. At least five distinct peaks can be clearly observed in the methine and carbonyl resonances, three of them closely spaced in each of the resonances. The methyl resonance also comprises at least two closely spaced peaks and one separate peak. The five distinct peaks represent five crystallographically inequivalent sites in the α (10_3) crystalline form. These may be compared to the NMR spectra of isotactic polypropylene wherein the two individual peaks have been assigned to different crystallographic sites which have distinct nuclear environments in the crystalline domains of the polymer.[25−27] Since only stress-induced crystallinity has been shown to form the β (3_1) crystalline form in PLLA,[5,16,17] we do not expect the β form to be present in these quiescently crystallized PLLA samples.

The carbonyl resonance, due to its narrower and well-separated peaks, can easily be resolved into five narrow Lorentzian peaks and a broad Gaussian peak. The Lorentzian peaks represent the crystalline component, while the Gaussian peak corresponds to the amorphous content in the sample. The fraction of polymer chains in the folds and in between the lamellae also contribute

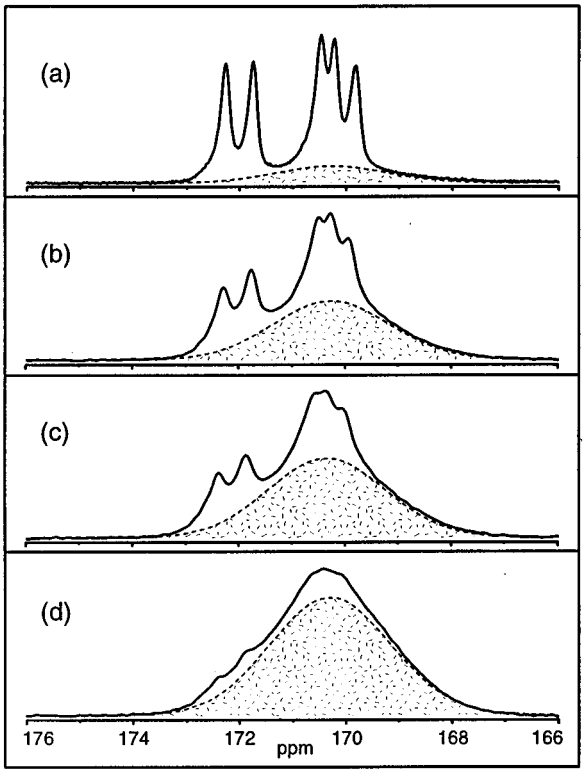

Figure 4. Carbonyl resonance in the ^{13}C CP-MAS spectra of partially crystalline (a) <0.1% *R* PLLA, (b) 1.6% *R* PLLA, (c) 3.2% *R* PLLA, and (d) 6.3% *R* PLLA. The shaded area is the approximate contribution from the amorphous content in each polymer.

to this amorphous component. The width and position of the Gaussian peak matches the carbonyl resonance of the amorphous polymer. Since the cross-polarization efficiency is identical in the amorphous and crystalline domains of the polymer (*vide infra*), the normalized integrated area of the resolved peaks represents the fraction of molecules in that particular environment.

Several experiments were performed to compare the cross-polarization efficiency for the crystalline and amorphous domains in the polymer. They were assumed to be identical on the basis of the following results. (1) The plots of integrated intensity *vs* the contact time for amorphous and partially crystalline PLLA were identical within the errors in the NMR measurement. Since the CP-MAS measurements were made at about 35 °C below the T_g of the polymer, the mobility differences (in the kilohertz regime) are expected to be minimal. (2) The shape of the resonances in the spectra of partially crystalline PLLA did not change with varying contact times. (3) The integrated intensity of the various partially crystalline and amorphous polymers was found to be proportional to the weight of the polymer in the rotor when identical instrumental conditions were employed. (4) The ^1H T_1 time for all samples was between 0.94 and 1.11 s, shorter for amorphous and longer for crystalline PLLA. Rapid ^1H spin diffusion may be responsible for only one T_1 time observed for each of the samples.

Figure 4 shows the carbonyl resonance in the ^{13}C CP-MAS NMR spectrum of various melt-crystallized PLLA polymer samples with increasing % *R* content. The shaded area depicting a broad Gaussian peak in each of the carbonyl resonances indicates (approximately) the amorphous content in the samples. The spectrum of highly crystalline (<0.1% *R*) PLLA in Figure 4a indicates the presence of only 10% amorphous component. Since this 10% includes contributions from both partially ordered chain folds on the surface of the lamellae and disordered amorphous domains between the lamellae and between the spherulites, it is an upper limit for the amorphous component between the lamellae. The spectra of other partially crystalline PLLA (Figure 4b,c) are similar to the spectra of poly(L-lactide) and poly(D-lactide) published previously.[25,26,28]

There are two additional features apparent from the spectra shown in Figure 4. First, the percent amorphous content increases with increasing % *R* lactide content, and second, the crystalline resonances appear to broaden with decreased crystallinity and higher % *R* content. The increase in amorphous content is not surprising since it is known that poly(D,L-lactide) does not crystallize and an increase in *R* stereoconfiguration defect sites will increasingly inhibit crystallization of the predominantly *S* stereoconfigured lactide units in PLLA. Determining the cause of the broadening of the crystalline resonances with increasing amorphous content and % *R* content is more difficult. One explanation is that the lactide repeat units in the polymer possess *anisotropic bulk magnetic susceptibility* (ABMS)[27] due to the presence of carbonyl groups. Within each spherulite, there is sufficient order for an approximate inversion symmetry at the micrometer level. Upon rotation, as in MAS, the bulk magnetic susceptibility of the spherulite will remain almost constant. However in the surrounding amorphous domains, the disordered orientation of the repeat units will continuously change the bulk magnetic susceptibility with rotation of the sample. This ABMS of the amorphous component will affect the lattice molecules near the surface of the spherulites and can broaden the crystalline resonances. This effect may be compared to the broadening of the adamantane peaks in a mixture of adamantane and hexamethylbenzene, as shown by VanderHart *et al.*[29] The presence of *isotropic bulk magnetic susceptibility* differences are not expected to affect the spectra since they are averaged out by the magic-angle spinning.[29] It is unclear whether relative amounts of crystalline and amorphous domains or the spherulite shape and size have a significant broadening effect. Another explanation for a correlation between broadening and increasing % *R* content may be a change in the lamellar thickness and composition. The lamellar thickness is expected to be related directly to the L-lactide content in the polymer. For the lack of a better measurement, the L-lactide content can be equated to the %*S* content, i.e. (100 − % *R*) content. Since the width of the crystalline resonance is inversely related to the lamellar thickness, this is one possibility for correlation between broadening and % *R* content. In addition, it is possible that a fraction of the -*R*- and -*RR*- defect sites in the predominantly -*SSSSS*- PLLA get trapped within the crystalline domains. These defect sites would reduce the order in the crystalline domains and induce the broadening of their resonance. A higher % *R* content could mean more defects incorporated and consequently a broader resonance observed. Further experiments are in progress to determine whether some fraction of the -*R*- and -*RR*- defect sites are incorporated into the crystalline lattice.

Parts a−c of Figure 5 show the change in the carbonyl CP-MAS resonance of 1.6% *R*, 3.2% *R*, and 6.3% *R* PLLA, respectively, when either 0%, 1%, or 10% talc is present in the three polymers. With the exception of

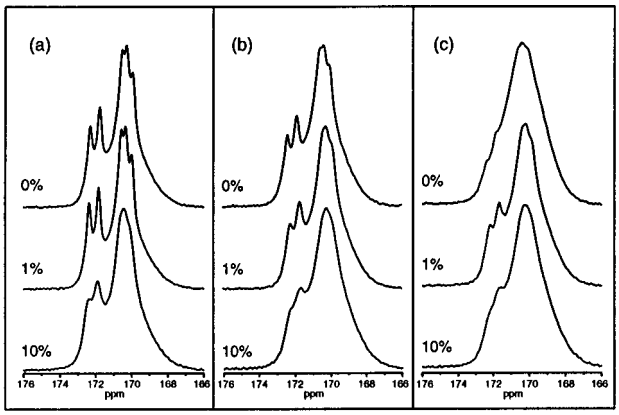

Figure 5. Carbonyl resonance in the ^{13}C CP-MAS spectra of partially crystalline (a) 1.6% *R* PLLA, (b) 3.2% *R* PLLA, and (c) 6.3% *R* PLLA with the presence of either 0%, 1%, or 10% talc in the three polymers. All samples were subject to similar thermal treatments.

the (6.3% *R* PLLA + 1% talc) sample, for each of the polymer compositions, the crystalline resonances broaden with increasing talc content. Addition of talc can promote crystallization by providing additional nucleation sites. This increased nucleation density usually results in smaller spherulite size. The molecules at the surface of the spherulites and at the surface of the talc nucleation site have a nonuniform local environment. So, if the number of crystalline lattice molecules near the surface of the spherulites and at the surface of talc particles are comparable to those in the bulk of the spherulites, broadening of the crystalline resonances is expected (proportional to radius^{-1}). The cause for narrowing of the crystalline resonance with presence of 1% talc in 6.3% *R* PLLA is unclear. The increased order may be speculated to be either due to formation of symmetric spherulites instead of nonsymmetric spherulites or due to fewer defect sites incorporated into the crystalline domains.

The results shown in Figures 4 and 5 indicate a correlation between the morphology of the polymer (lamellar thickness, defect sites, additives, etc.) and the broadening of the crystalline resonances observed in the NMR spectrum. In order to test whether spherulite size affects the line widths, six additional samples were prepared under highly controlled conditions (Table 2). Thin films were also prepared under identical conditions, and their macroscopic morphology (spherulite size) was determined by polarized microscopy. Since in these samples the composition of the polymer and temperature of crystallization was maintained to be identical, their lamellar thickness is expected to be similar. Figure 6 shows the morphology of (a) melt-crystallized 1.6% *R* PLLA, (b) quench/annealed 1.6% *R* PLLA, (c) melt-crystallized (1.6% *R* + 1% talc) PLLA, and (d) quench/annealed (1.6% *R* + 1% talc) PLLA. The size of each of the polarized microscope pictures is approximately 215 μm × 145 μm. The spherulites in the melt-crystallized 1.6% *R* PLLA are intertwined and have the largest size (~15 μm) among the six samples (Figure 6a). The spherulite size in melt-crystallized (1.6% *R* + 1% talc) PLLA ranges from 1 to 10 μm (Figure 6c). The talc acts as a nucleating site during crystallization, causing more spherulites with smaller size to be formed. The quench/annealed 1.6% *R* PLLA without talc also has a similar morphology (1−10 μm) (Figure 6b). On the other hand, quench/annealed (1.6% *R* + 1% talc) PLLA has tiny spherulites (<0.1 μm) (Figure 6d). The quenched samples showed no crystallization, and

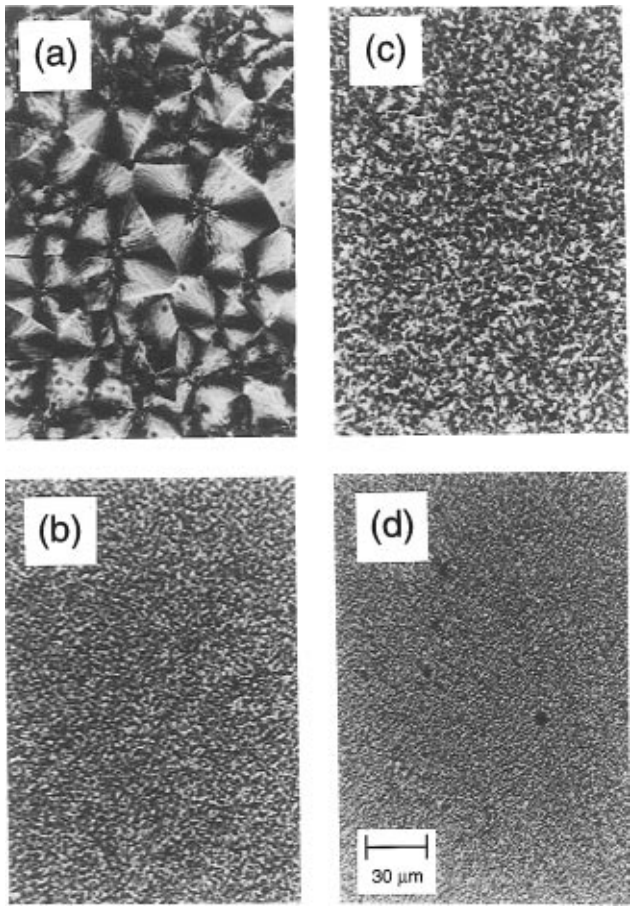

Figure 6. Morphology of thin films of (a) melt-crystallized 1.6% *R* PLLA, (b) quench/annealed 1.6% *R* PLLA, (c) melt-crystallized (1.6% *R* PLLA + 1% talc), and (d) quench/annealed (1.6% *R* PLLA + 1% talc) photographed using a polarized microscope. The size of each of the pictures is approximately 215 μm × 145 μm.

hence their polarized microscope pictures are not shown. The ΔH_{cryst} values obtained by DSC for a−d samples are 53, 43, 52, and 38 J/g, respectively.

The carbonyl resonance in the NMR spectra and the spectral fits obtained using the *linear combination fit* procedure are shown in Figure 7 for the four samples, (a) melt-crystallized 1.6% *R* PLLA, (b) quench/annealed 1.6% *R* PLLA, (c) melt-crystallized (1.6% *R* + 1% talc) PLLA, and (d) quench/annealed (1.6% *R* + 1% talc) PLLA. The details of the *linear combination fit* procedure are described in the Experimental Section. A poor fit of the fine structure in the closely separated peaks is an artifact of the way the peaks were artificially broadened. The line shapes of the narrow crystalline peaks are expected to gain Gaussian character when broadened but the "moving average" in the fit is only an approximation to Gaussian broadening. The spacing between each data point was 30300 Hz/32 768 points ≈ 0.925 Hz. Samples b and c had similar average spherulite size, and required similar broadening (±10 points) of the crystalline resonance. Sample a had the largest spherulite size and required the least broadening (±8 points), while sample d had the smallest spherulite size and used the most broadening (±12 points) for the fit.

If the lamellar thicknesses in these four samples are identical, as noted earlier, the only morphological difference expected between (a) and (b), and between (c) and (d) is the nucleation density and spherulite size. The NMR spectra appear to reflects this difference as broadening of the crystalline resonance. We cannot rule

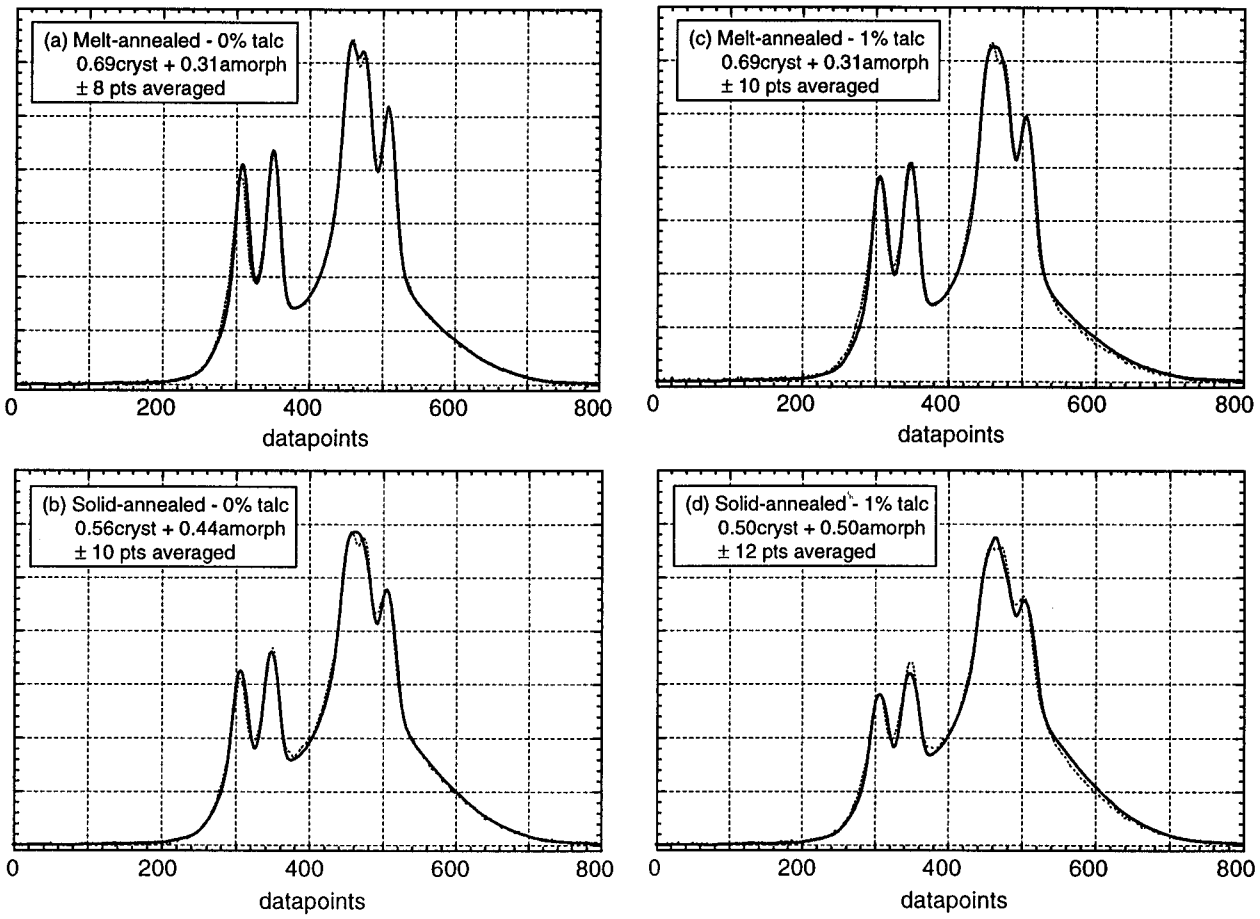

Figure 7. Carbonyl resonance in ^{13}C CP-MAS spectra (dashed line) and the fit (solid line) generated using a linear combination of amorphous and artificially broadened crystalline resonances in (a) melt-crystallized 1.6% *R* PLLA, (b) quench/annealed 1.6% *R* PLLA, (c) melt-crystallized (1.6% *R* PLLA + 1% talc), and (d) quench/annealed (1.6% *R* PLLA + 1% talc).

out the possibility of a difference in lamellar thickness in the two sets of samples contributing to the broadening. However, since experimental measurement of lamellar thickness in these four samples is currently unavailable, and the sensitivity of peak widths to changes in lamellar thickness is not known, we suspect that the broadening may due to ABMS of randomly oriented amorphous domains surrounding the spherulites. For comparison, consider the effect of hexamethylbenzene (HMB) on the resonance of adamantane crystals of different sizes. In a test experiment, the peak width of the adamantane resonance in a 10% by weight mixture with HMB was 33 Hz compared to 3 Hz for pure adamantane. When the adamantane was first ground using mortar and pestle to form smaller sized crystals and then mixed with HMB in the same 1:9 ratio by weight, the peak width of its resonance increased to 50 Hz. Hence, the extent of ABMS broadening is expected to be inversely related to the size of the crystals. The adamantane crystal, which is cubic and possesses an isotropic bulk magnetic susceptibility tensor,[29] may be compared to a symmetric PLLA spherulite which, as mentioned earlier, should have only minor fluctuations in its bulk magnetic susceptibility. However, the broadening effect due to ABMS of the amorphous PLLA will not be as pronounced as in the case of HMB crystals. The evaluation of a possible nonlinear relationship between the spherulite size and broadening was not explored any further. Nonetheless, if the broadening is related to the surface area of the spherulites, it would be inversely proportional to the average radius of the spherulites. Additional experiments are being considered to conclusively identify the extent of broadening caused by ABMS of the amorphous PLLA.

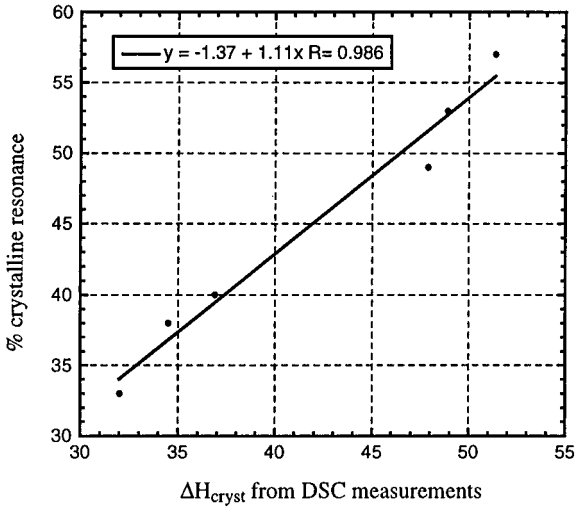

Figure 8. Correlation plot of the percent crystallinity values determined using the *linear combination fit* with the ΔH_{cryst} values obtained using DSC for various partially crystalline 1.6% *R* PLLA and 3.2% *R* PLLA samples listed in Table 1.

The DSC values of ΔH_{cryst} correlate reasonably well with the percent fraction of crystalline resonance determined by the *linear combination fit*. These are plotted in Figures 8 and 9 for a few of the PLLA samples listed in Tables 1 and 2, respectively. Here, the values for 6.3% *R* PLLA samples were not used due to unre-

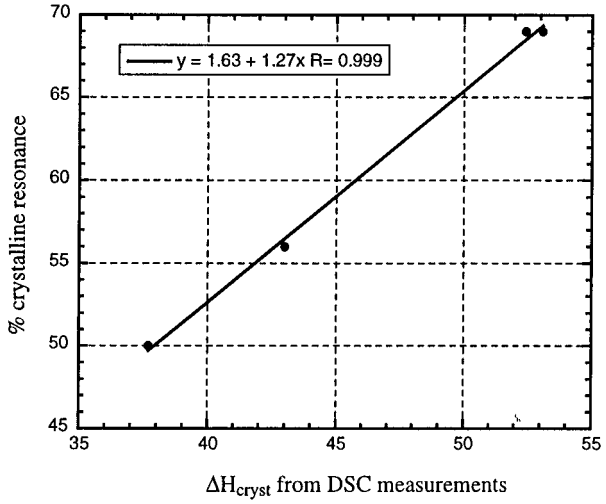

Figure 9. Correlation plot of the percent crystallinity values determined using the *linear combination fit* with the ΔH_{cryst} values obtained using DSC for various 1.6% *R* PLLA samples listed in Table 2.

liability of the fit and possible differences in the correlation between the ΔH values obtained by DSC and the percent crystallinity in the polymer. The spectra for samples listed in Table 2 and the reference spectra of highly crystalline and amorphous PLLA used for the linear combination fit procedure were acquired under identical instrumental conditions. However, the spectra of the samples listed in Table 1 (except no. 1) were acquired on various days under nonidentical conditions. This may result in additional subjective error in the crystallinity values determined by the linear combination fit method for samples in Table 1.

The error associated with estimation of percent crystallinity by the *linear combination fit* procedure may by evaluated by observing the spectral fit simulated with nonoptimal parameters. For example in Figure 10, the carbonyl resonance of melt-crystallized 1.6% *R* PLLA (sample no. 2 in Table 2) and four simulated fits with nonoptimal parameters are displayed. Instead of a crystalline resonance fraction of 69% and broadening with ±8 data points (Figure 7a), the simulation in (i) has 64% crystalline resonance fraction and ±8 data point broadening and (ii) has 74% crystalline resonance and ±8 data point broadening. The simulation of the base of the resonance around data point no. 550 and around data point no. 400 fits poorly in (i) and (ii). The effect of nonoptimal broadening is shown in (iii) and (iv) for averaging with ±6 data points and ±10 data points, respectively, instead of the optimal ±8 data points. The width of the pair of peaks around data point no. 325 is poorly fit in (iii) and (iv).

We have demonstrated that ^{13}C CP-MAS NMR spectra can be used to determine the crystallinity in PLLA samples. In addition, it may be possible to estimate the average morphology in the polymer if the lactide composition of the polymer is known and the effect of additives has been accounted for. For a simple correlation between integrated intensity and the molecules in various domains, the measurement must be made at temperatures below the T_g of the polymer so that differences in mobility between the amorphous and crystalline domains are minimal. It should also be

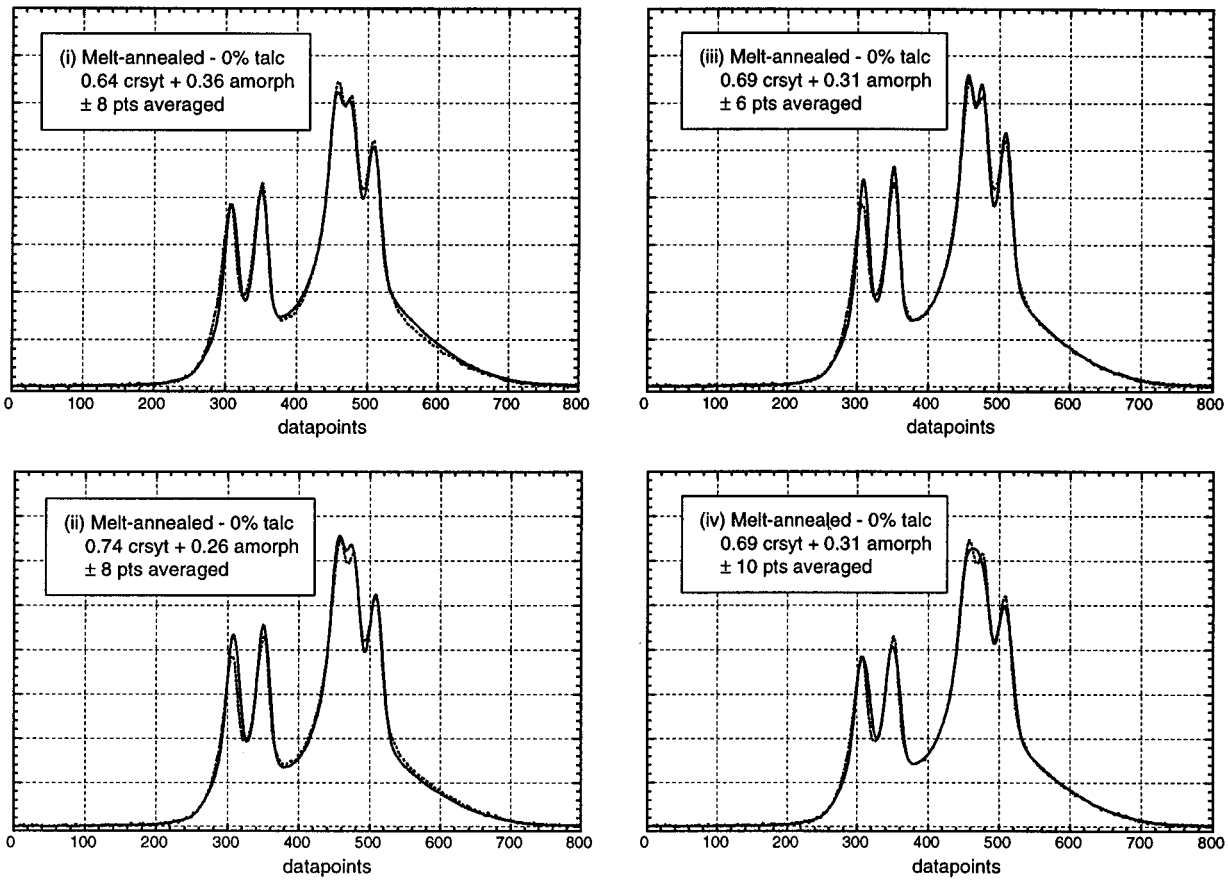

Figure 10. Carbonyl resonance in ^{13}C CP-MAS spectra (dashed line) and the fit (solid line) generated using the *linear combination fit* procedure for melt-crystallized 1.6% *R* PLLA with *nonoptimal* parameter values of (i) 64% crystalline resonance fraction and ±8 data points averaged, (ii) 74% crystalline resonance fraction and ±8 data points averaged, (iii) 69% crystalline resonance fraction and ±6 data points averaged, and (iv) 69% crystalline resonance fraction and ±10 data points averaged.

noted that the peak widths and line shapes are extremely sensitive to positioning of the rotor accurately at the magic angle with respect to the static magnetic field (B_0). Any misalignment of the rotor introduces distortion in the carbonyl peaks from incomplete averaging of the chemical shift anisotropy. The resolution of the NMR spectrometer, which is affected by a number of factors including the homogeneity of the field, also affects the peak widths of the narrow crystalline resonances. These instrumental issues may have minimal effect in the analysis as long as the spectrum of the highly crystalline sample is also acquired under identical conditions. Possible factors affecting the crystalline peak widths include (1) lamellar thickness and composition, which may depend on crystallization temperature and the presence of impurities of D-lactide and *meso*-lactide in the poly(L-lactide), (2) presence of additives like talc, and (3) spherulite shape and size. Further experiments are in progress to evaluate the extent of effect of each of these factors.

Conclusion

Solid-state NMR has been successfully used to measure the percent crystallinity in partially crystalline PLLA samples. In favorable cases, it may be possible to estimate the morphology of the crystalline domains in the PLLA. The *short-range* order (nanometer) as well as *long-range* order (micrometer) in PLLA appears to affect the ^{13}C CP-MAS spectrum. A simple method which can be used to extract the information of crystallinity and morphology from the NMR spectra was discussed.

Acknowledgment. This work was supported by a NIST ATP grant to Cargill Incorporated. The authors thank Eric Hall at Cargill Corn Milling EcoPLA Development for providing helpful advice and some of the polymer samples for this study and Jeffrey Kolstad at Cargill Central Research for fruitful discussions. In addition, we gratefully acknowledge the contributions from the reviewers in improving and clarifying the concepts in this paper.

References and Notes

(1) Vert, M.; Schwarch, G.; Coudane, J. *J. Macromol. Sci., Pure Appl. Chem.* **1995**, *A32*, 787−796.
(2) Sorensen, W. R.; Campbell, T. W. *Preparative Methods of Polymer Chemistry*; Wiley: New York, 1961.
(3) Kleine, J.; Kleine, H. H. *Makromol. Chem.* **1959**, *30*, 23.
(4) Schulz, V. C.; Schwaab, J. *Makromol. Chem.* **1965**, *87*, 90−102.
(5) De Santis, P.; Kovacs, A. J. *Biopolymers* **1968**, *6*, 299−306.
(6) Tonelli, A. E.; Flory, P. J. *Macromolecules* **1969**, *2*, 225.
(7) Schindler, A.; Harper, D. *Polym. Lett. Ed.* **1976**, *14*, 729−734.
(8) Chabot, F.; Vert, M.; Chapelle, S.; Granger, P. *Polymer* **1983**, *24*, 53−59.
(9) Tsuji, H.; Ikada, Y. *Polymer* **1995**, *36*, 2709−2716.
(10) Brochu, S.; Prud'homme, R. E.; Barakat, I.; Jérome, R. *Macromolecules* **1995**, *28*, 5230−5239.
(11) Tsuji, H.; Ikada, Y. *J. Appl. Polym. Sci.* **1995**, *58*, 1793−1802.
(12) Boenig, H. *Structure and Properties of Polymers*; John Wiley and Sons: New York, 1973.
(13) Hoffman, J. D.; Davis, G. T.; Lauritzen, J. J. I. In *Treatise on Solid State Chemistry*; Hannay, N. B., Ed.; Plenum Press: New York, 1976; Vol. 3, pp 497−614.
(14) Remarks of a reviewer.
(15) Sanchez, I. C.; Eby, R. K. *J. Res. Natl. Bur. Stand. (U.S.)* **1973**, *77A*, 353−358.
(16) Hoogsteen, W.; Postema, A. R.; Pennings, A. J.; ten Brinke, G. *Macromolecules* **1990**, *23*, 634−642.
(17) Okihara, T.; Tsuji, M.; Kawaguchi, A.; Katayama, K. *J. Macromol. Sci.,Phys.* **1991**, *B30*, 119−140.
(18) Perego, G.; Cella, G. D.; Bastioli, C. *J. Appl. Polym. Sci.* **1996**, *59*, 37−43.
(19) Tang, P.; Reimer, J. E.; Denn, M. M. *Macromolecules* **1993**, *26*, 4269−4274.
(20) Mathias, L. J.; Johnson, C. G.; Steadman, S. J. *SPIE* **1993**, *1916*, 309−319.
(21) O'Connell, E. M.; Peiffer, D. G.; Root, T. W.; Cooper, S. L. *Macromolecules* **1996**, *29*, 2124−2130.
(22) Lathrop, D. A.; Gleason, K. K. *Mater. Res. Soc. Symp. Proc.* **1994**, *321*, 155−160.
(23) Lathrop, D. A.; Gleason, K. K. *Macromolecules* **1993**, *26*, 4652−4657.
(24) Sullivan, M. J. *Macromol. Symp.* **1994**, *86*, 145−159.
(25) Howe, C.; Vasanthan, N.; MacClamrock, C.; Sankar, S.; Shin, I. D.; Simonsen, I. K.; Tonelli, A. E. *Macromolecules* **1994**, *27*, 7433−7436.
(26) Howe, C.; Sankar, S.; Tonelli, A. E. *Polymer* **1993**, *34*, 2674−2676.
(27) Gomez, M. A.; Hajime, T.; Tonelli, A. E. *Polymer* **1987**, *28*, 2227−2232.
(28) Tsuji, H.; Horii, F.; Nakagawa, M.; Ikada, Y.; Odani, H.; Kitamaru, R. *Macromolecules* **1992**, *25*, 4114−4118.
(29) VanderHart, D. L.; Earl, W. L.; Garroway, A. N. *J. Magn. Reson.* **1981**, *44*, 361−401.

MA960828Z